

An Extremely Red Nucleus in an Absorbed QSO at $z = 0.65$

Masayuki AKIYAMA*

Subaru Telescope, National Astronomical Observatory of Japan,

650 North A'ohoku Place, Hilo, HI, 96720, U.S.A

E-mail(MA): akiyama@naoj.org

and

Kouji OHTA*

Department of Astronomy, Faculty of Science, Kyoto University, Kyoto 606-8502

E-mail(KO): ohta@kusastro.kyoto-u.ac.jp

(Received 2000 August 30; accepted 2000 October 30)

Abstract

The results of K -band-imaging observations of a candidate of an absorbed QSO at $z = 0.653$, AX J131831+3341, are presented. The $B - K$ color of the object is 4.85 mag, which is much redder than optically-selected QSOs. The K -band image shows nuclear and extended components, the same as in the optical V -, R -, and I -band images. The nuclear component ($I - K = 4.29$ mag) is much redder than the power-law models with energy indices of 0 to -1.0 , which well reproduce the $V - R$ and $R - I$ optical colors of the nuclear component. A heavily absorbed ($A_V \sim 3$ mag) nucleus may emerge in the K -band, while optical light may originate from scattered nuclear light. The $I - K$ color of the extended component is 2.2 mag, which is consistent with the post-starburst nature of the host galaxy, which is also suggested from the $V - R$ and $R - I$ colors of the extended component.

Key words: galaxies: active — galaxies: individual (AX J131831+3341) — galaxies: photometry — quasars

* Visiting astronomer of the University of Hawaii 88" telescope.

1. Introduction

X-ray-selected absorbed radio-quiet QSOs are a new population of AGNs which have appeared in recent deep X-ray surveys (Almaini et al. 1995; Ohta et al. 1996; Kim, Elvis 1999; Fiore et al. 1999). Although their X-ray luminosities reach those of QSOs, the absence of a strong broad Balmer emission line or their large Balmer decrements of broad emission lines suggests the existence of strong absorption to their nuclei. These objects are considered to be the long-sought luminous cousins of the type-2 Seyfert galaxies, in other words, an absorbed version of broad-line non-absorbed QSOs. Their optical and near-infrared colors are normally redder than optically-selected non-absorbed QSOs (Georgantopoulos et al. 1999; Nakanishi et al. 2000). The origin of their red colors is thought to be an absorbed nuclear continuum or that from a host galaxy of the QSO.

AX J131831+3341 is another candidate of an absorbed radio-quiet QSO at a redshift of 0.653 found during the course of the optical identification of hard X-ray sources in the ASCA Large Sky Survey (LSS; Akiyama et al. 2000a, hereafter Paper I). Its X-ray luminosity is estimated to be $\sim 10^{45}$ erg s $^{-1}$. Deep R - and V - band images reveal the presence of a point-like nucleus and an extended component (Akiyama et al. 2000b, hereafter Paper II). The R -band magnitude of the nuclear component is much fainter than that expected from the observed X-ray flux with optical to X-ray flux ratios of X-ray-selected broad-line QSOs. The optical faintness suggests that the nucleus is absorbed with A_V of larger than 3 mag. However, the optical $V - R$ and $R - I$ colors of the nuclear component are as blue as a power-law model with an energy index of $\alpha = -1$ ($f_\nu \propto \nu^\alpha$). Although the colors are slightly redder than the averaged color of QSOs ($\alpha = -0.3$ – -0.5 , Francis et al. 1996), an absorption of only $A_V \leq 1$ mag is required to reproduce the colors. Thus, the optical colors conflict with the amount of absorption to the nucleus, estimated from the optical faintness. Another important property of this object is that a broad Mg II 2800 Å emission line is seen in the optical spectrum (Paper I). Therefore, in order to explain all of these properties simultaneously, the origin of the optical nuclear component is strongly suggested to be a scattered nuclear light and the nuclear emission is heavily absorbed ($A_V \geq 3$ mag), though there is a possibility that the nuclear component is a slightly absorbed ($A_V \sim 1$ mag) nucleus, if its intrinsic X-ray to optical flux ratio is the largest among X-ray-selected broad-line QSOs (Paper II). The scattered nuclear light should contain a broad H β emission line as well as the broad Mg II 2800 Å emission line. The absence of the broad H β emission line in the optical spectrum (Paper I) can be caused by contamination of the host galaxy continuum, because the extended component contributes to 50% of the I -band

light in a $1.''2$ circular aperture, which corresponds to a slit width of $1.''2$. In order to investigate the near-infrared to optical spectral energy distribution of the object, and to unveil the origin of the near-infrared to optical continuum component, we conducted a K -band imaging observation. Throughout this paper we use $q_0 = 0.5$ and $H_0 = 50 \text{ km s}^{-1} \text{ Mpc}^{-1}$.

2. Observations

The K -band imaging observations were made with a QUick InfraRed Camera (QUIRC) with a 1024×1024 HgCdTe Astronomical Wide Area Infrared Imaging (HAWAII) array attached to the $f/10$ focus of the University of Hawaii $88''$ telescope on 2000 March 21 and 22. Sixteen and twenty-eight frames with an exposure time of 180 s were taken on March 21 and 22, respectively, with small offsets of the telescope pointing. The pixel scale of the camera was $0.''189 \text{ pixel}^{-1}$. The seeing condition during the observation was FWHM of stars of $\sim 0.''9$ and $\sim 1.''2$ in the first and second nights, respectively. During the observing run, UKIRT faint standard stars (FS 121, FS 124, FS 129, FS 126, FS 132, FS 137, and FS 135) were observed for a photometric calibration. For each star, we took at least 3 images, while changing the position of the star on the detector to reduce any systematic errors.

The data reduction was performed as follows: at first, we made sky-background frames by stacking object frames of each night without a shift. The sky-background frame of the same night was subtracted from each object frame. Next, flat-fielding was performed with a dome-flat frame. Finally, after correcting the offset of each object frame, we combined 11 and 19 object frames taken under a good seeing condition in the first and second night, respectively. Sky-subtraction and flat-fielding were also performed for standard star frames in the same manner, though we did not shift and combine the standard star frames. The counts of the standard star in each frame were measured individually by using a growth curve-fitting method for each star. Based on the scatters of the count rate to the magnitude conversion factors derived from the observed UKIRT faint standard stars, we estimated the uncertainties of the photometric calibrations as 0.05 mag for the first night data and 0.1 mag for the second night data. The uncertainty includes those of the flat-fielding.

3. Results

3.1. Morphology and Total Magnitude

The K -band image made from the first and the second night data is shown in figure 1. AX J131831+3341 shows a point-like nucleus and an extended component, just as in the optical image in Paper II. The profile of the nuclear component is consistent with that of stars in the image. The standard deviation in the sky region of the image is 7 counts per pixel, which corresponds to $22.2 \text{ mag arcsec}^{-2}$ in the K band. In figure 1, we show a sky-subtracted image of the object with the surface brightness ranging from -3 times the standard deviation to $+10$ times the standard deviation as a gray scale with a linear scale.

We measured the total magnitude of AX J131831+3341 in a $26.''4$ aperture centered on the nucleus, excluding objects around AX J131831+3341 and a knot in the northwestern direction, as we did for the optical images in Paper II. The resulting K -band magnitudes are $16.38 \pm 0.14 \text{ mag}$ and $16.28 \pm 0.16 \text{ mag}$ from the first and the second night data, respectively. The uncertainty of the magnitude includes that of the photometric calibration and that of the sky determination (0.13 mag). The two magnitudes agree with each other within the uncertainty. The resulting $B - K$ color of AX J131831+3341 is $4.95 \pm 0.17 \text{ mag}$; it is as red as other X-ray-selected absorbed QSOs ($B - K = 5.4 \text{ mag}$ for RX J13334+0001 at $z = 2.35$, Georgantopoulos et al. 1999; $B - K = 5.3 \text{ mag}$ for AX J08494+4454 at $z = 0.9$, Akiyama et al. in preparation). In the next section, we estimate the magnitudes and colors of the nuclear and the extended components separately.

3.2. Colors and Magnitudes of the Extended and the Nuclear Components

In order to evaluate the colors of the extended component, we measured the magnitude in regions A and B ($4.''8 \times 3.''6$ and $2.''4 \times 3.''6$) shown in figure 1. These regions are the same as those used for the optical images in Paper II. Because the data taken during the first night have a smaller seeing size, and the size is not so much different from that of the optical images ($0.''7 \sim 0.''8$), we use only the first-night data for the color measurements. The magnitude in region A (B) was measured to be 18.56 (18.43) mag. The uncertainty of the photometry is estimated to be 0.11 mag , which includes the uncertainties of the photometric zero point and the sky determination (0.1 mag). Thus, the color in region A (B) is $I - K$ of 2.54 (2.49) $\pm 0.19 \text{ mag}$.

To derive the K -band magnitude of the nuclear component, we deconvolved the nuclear and extended components, following the same method as used in the deconvolution of the V -, R -, and I -band images (Paper II). Since the object has an asymmetric, complex feature, in order to obtain a rather symmetric and smooth brightness distribution, we,

at first, modeled the surface-brightness distribution of the galaxy by fitting ellipses, of which the centers, position angles, ellipticities, and surface brightnesses were free parameters, to the isophotes of the object. We adopted the same sampling steps as those used for the optical images; the step size was taken to be one twelfth of the semi-major length of each ellipse. The constructed model and the residual image after subtracting the model from the original image are shown in figures 1b and 1c. (All images in figure 1 are shown in the same count-rate range.) The model well describes the overall shape of the original image. The surface-brightness profiles were derived as sections of the model image along the major-axis (position angle of 114°), and are shown in figure 2 by the thick solid lines. We fit the profiles with a model consisting of a nuclear component (a point source) and an exponential disk component. The profile of the point-spread function was determined by applying the same profile measuring method as that applied for the object to the three stars, one of which was the reference star for the frame alignment. We assumed that the scale length of the exponential disk in the K band was the same as that in the R -band image, and left the normalizations of the point source and the exponential disk as free parameters. The best-fit normalizations were determined from profiles between $2''$ and $3''$ where the exponential disk component dominates the profile and within $1''$ where the nuclear component dominates the profile. The summed profiles of the best-fit models are shown by the thick dashed lines in figure 2. The model well describes the profile of the object in both directions. The resulting magnitude of the nuclear component is 17.48 mag and the central surface brightness of the extended component is 20.00 (19.82) mag arcsec^{-2} in the southeastern (northwestern) profile. We plot models whose normalizations of the nuclear component and the extended component are changed by ± 0.2 mag by the thin solid lines. Because most of the observed profiles run between these thin profiles, the uncertainties of the parameters are estimated to be less than ± 0.2 magnitude. Subtracting the magnitude of the nuclear component from the total magnitude, we obtain the magnitude of the extended component as 16.87 ± 0.25 mag. As a result, the $I - K$ color of the extended component was calculated to be 2.17 ± 0.30 .

4. Discussions

4.1. Red Nuclear Component

The $I - K$ and $R - I$ colors of the nuclear component are plotted in figure 3 (filled square). The $I - K$ color of the nuclear component is 4.29 ± 0.25 mag. It is much redder than those of optically selected QSOs at redshifts of between

0.2 and 1.5 (open squares in figure 3 from Elvis et al. 1994), and is also much redder than those of the power-law continuum with energy indices of 0 to -1.0 (open pentagons in figure 3), which reproduce the $V - R$ and $R - I$ colors of the nuclear component well with no or a slight extinction. Since a reddening of the power-law continuum cannot explain the red color appearing in figure 3, this $I - K$ color can be explained by neither the scattered nuclear light nor slightly absorbed nuclear emission. In the K band, a contribution from another continuum emission, which is at least ~ 5 -times brighter than the optical power-law component in the rest frame $1.3 \mu\text{m}$, is required. Candidates of such components are heavily absorbed direct nuclear emission, dust thermal emission, relativistically beamed synchrotron emission, and host galaxy emission.

One possible origin is that a heavily absorbed red nucleus emerges in the K -band. Since the component must dominate the K -band flux, but must not contribute significantly to the I -band flux, an absorption larger than $A_V = 3$ mag in the rest frame is required. The amount of the absorption is within the range derived from the X-ray spectrum of the object ($A_V = 1 - 6$ mag). Based on the observed K -band magnitude of the nuclear component, the A_V of 3 mag in the rest frame ($A_K = 0.9$ mag in the observed frame), and the typical energy index of the QSO optical power-law continuum ($\alpha = -0.5$, i.e., $V - K = 2.68$ mag), the absorption corrected V -band magnitude of the nucleus is expected to be 18.9 mag. This leads to an intrinsic absorption-corrected X-ray to optical flux ratio, $\log(f_{X_{0.3-3.5\text{keV}}}/f_V)$, of $+0.83$. The value is within the range of the X-ray to optical flux ratio of AGN sample of Einstein Medium Sensitivity Survey [$\log f_{X_{0.3-3.5\text{keV}}}/f_V = -1.0 - +1.4$] (Stocke et al. 1991). Therefore, it is plausible that the nucleus is heavily absorbed ($A_V \sim 3$ mag) and emerges only in the K band, while in the optical wavelength we see the scattered blue nuclear emission. Comparing the observed V -band magnitude of the nuclear component ($V = 22.61$ mag, Paper II) with the absorption corrected V -band magnitude of the nucleus, we estimated the fraction of the scattered component as 2%, which is similar to that observed in radio galaxies (Alighieri et al. 1994).

The other possible origin for the red $I - K$ color is thermal emission by hot dusts in the K band. The dust thermal emission with a temperature of $1300 - 1500$ K starts to contribute to the continuum of QSOs at $1.0 \mu\text{m}$ (Pier, Krolik 1993; Kobayashi et al. 1993). The K -band nuclear component is at least ~ 5 -times brighter than that expected from the optical power-law continuum component at rest-frame $1.3 \mu\text{m}$. This value is much larger than the estimated contribution by the dust thermal emission at $1.3 \mu\text{m}$: less than 1 (Pier, Krolik 1993) and less than 2 (Kobayashi et al. 1993).

For red quasars found in the Parkes flat-spectrum radio source survey, a relativistically beamed synchrotron

component is proposed as the origin of the red colors (Serjeant, Rawlings 1995; Srianand, Kembhavi 1997; Francis et al. 2000). However, because AX J131831+3341 has a radio-to-X-ray flux ratio similar to those of radio-quiet AGNs, the existence of such a strong synchrotron component is very unlikely.

It is possible that a stellar population in the nuclear region emerges in the K band. We plot the colors of the spectral evolution models of galaxies in figure 3. We use two models (Kodama, Arimoto 1997): 1) An elliptical model (plotted with a solid line) in which star formation occurs during the first 0.353 Gyr with an initial mass function with a slope of 1.20 and after that the galaxy evolves passively. The model parameters well reproduce the reddest and brightest ($M_V = -23$ mag) class elliptical galaxy in the Coma cluster (Kodama et al. 1998). 2) A disk model (plotted with a dotted line) in which star formation occurs constantly with the same initial mass function as the elliptical model. The colors of these models at ages from 0.01 Gyr to 12 Gyr at redshift of 0.653 are shown as tracks. We mark the positions at 6 Gyr age with tick marks on the tracks of both models. The age corresponds to that of the universe at a redshift of 0.653 under the adopted cosmological parameters of $q_0 = 0.5$ and $H_0 = 50 \text{ km s}^{-1} \text{ Mpc}^{-1}$. If we assume that the stellar population dominates the K -band light, but does not significantly contribute to the nuclear component in the I band (and the bluer bands), the stellar population must have a redder $I - K$ color than the observed $I - K$ color of the nuclear component. Without absorption, the reddest model ($I - K$ of 3.4 mag, an elliptical model with an age of 6 – 12 Gyr) is still bluer than the $I - K$ color of the nuclear component. Therefore, to reproduce the red $I - K$ color, at least absorption with A_V of 1 mag is required.

Such a red optical to near-infrared color and a blue optical color may be common characteristics of X-ray selected absorbed QSOs at intermediate redshifts. Recent observations reveal that another absorbed QSO at a redshift of 0.9, AX J08494+4454, also has a blue optical color and a red optical to near-infrared color ($R - I = 0.67$ mag and $I - K = 3.4$ mag, Nakanishi et al. 2000; Akiyama et al. in preparation). Also, a significant fraction of the optical and near-infrared counterparts of Chandra hard X-ray sources show similar red near-infrared colors ($I - HK' = 4\text{--}5$ mag) and blue optical colors ($B - I = 1\text{--}2$ mag) (Mushotzky et al. 2000).

4.2. Nature of the Extended Component

The extended component is thought to be the host galaxy of the QSO. The optical absolute magnitude of the component is similar to those of the brightest host galaxies of QSOs (Paper II). The $V - R$ and $R - I$ colors of the component are consistent with a 1 Gyr-old stellar population model without absorption. If we introduce optical

extinction ($A_V = 1\text{--}3\text{mag}$) in the host galaxy, the colors are also explained by a disk model at any ages or an elliptical at ages of less than 0.1 Gyr (Paper II).

The $I - K$ and $R - I$ colors of the extended component are plotted in figure 3 (filled circle). The colors agree with those of the 1 Gyr-old elliptical galaxy model. If we introduce an optical extinction, neither a disk model at any ages nor an elliptical model at ages of less than 0.1 Gyr can reproduce the $R - I$ and $I - K$ colors. Therefore the models involving the moderate absorption are rejected. Since a spectrum of the 1 Gyr-old elliptical model resembles that of a post-starburst galaxy, these colors may indicate that the host galaxy is in a post-starburst phase. The $I - K$ and $R - I$ colors measured in region B (filled pentagon) is also consistent with those of the 1 Gyr-old elliptical galaxy, but the $R - I$ color of region A (filled triangle) is bluer than that predicted by the model. Without extinction, the $R - I$ and $I - K$ colors of region A are not consistent with any galaxy models at ages less than 6 Gyr, which is a cosmic age at a redshift of 0.653. If we introduce an optical extinction in region A, the colors can be explained by a disk model at any ages with an absorption of $A_V = 1 - 3\text{ mag}$ or the elliptical model at ages of less than 0.1 Gyr with an absorption of $A_V \sim 3\text{ mag}$. Therefore, the colors of region A may reflect an obscured star-forming region in the host galaxy.

MA and KO appreciate support by K. Nakanishi and staff members of the UH observatory during the imaging observations. This research made use of the NASA/IPAC Extragalactic Database (NED), which is operated by the Jet Propulsion Laboratory, Caltech, under a contract with the National Aeronautics and Space Administration. MA acknowledges support from Research Fellowships of the Japan Society for the Promotion of Science for Young Scientists. KO's activity is supported by a grand-in-aid from the Ministry of Education, Science, Sports and Culture (11740123).

References

- Akiyama, M., Ohta, K., Tamura, N., Doi, M., Kimura, M., Komiyama, Y., Miyazaki, S., Nakata, F. et al. 2000b, PASJ, 52, 577 (Paper II)
- Akiyama, M., Ohta, K., Yamada, T., Kashikawa, N., Yagi, M., Kawasaki, W., Sakano, M., Tsuru, T. et al. 2000a, ApJ, 532, 700 (Paper I)
- Alighieri, S.S., Cimatti, A., & Fosbury, R.A.E. 1994, ApJ, 431, 123
- Almaini, O., Boyle, B. J., Griffiths, R. E., Shanks, T., Stewart, G. C., & Georgantopoulos, I. 1995, MNRAS, 277, 31
- Elvis, M., Wilkes, B.J., McDowell, J.C., Green, R.F., Bechtold, J., Willner, S.P., Oey, M.S., Polonski, E., & Cutri, R. 1994, ApJS, 95, 1
- Fiore, F., La Franca, F., Giommi, P., Elvis, M., Matt, G., Comastri, A., Molendi, S., & Gioia, I. 1999, MNRAS, 306, 55
- Francis, P.J. 1996, Proc. Astron. Soc. Australia, 13, 212
- Francis, P.J., Whiting, M.T., & Webster, R.L. 2000, Proc. Astron. Soc. Australia, 17, 56
- Georgantopoulos, I., Almaini, O., Shanks, T., Stewart, G.C., Griffiths, R.E., Boyle, B.J., & Gunn, K.F. 1999, MNRAS, 305, 125
- Kim, D.-W., & Elvis, M. 1999, ApJ, 516, 9
- Kobayashi, Y., Sato, S., Yamashita, T., Shiba, H., & Takami, H. 1993, ApJ, 404, 94
- Kodama, T., & Arimoto, N. 1997, A&A, 320, 41
- Kodama, T., Arimoto, N., Barger, A.J., & Aragón-Salamanca, A. 1998, A&A, 334, 99
- Mushotzky, R.F., Cowie, L.L., Barger, A.J., & Arnaud, K.A. 2000, Nature, 404, 459
- Nakanishi, K., Akiyama, M., Ohta, K., & Yamada, T. 2000, ApJ, 534, 587
- Ohta, K., Yamada, T., Nakanishi, K., Ogasaka, Y., Kii, T., & Hayashida, K. 1996, ApJ, 458, L57
- Pier, E.A., & Krolik, J.H. 1993, ApJ, 418, 673
- Serjeant, S., & Rawlings, S. 1995, Nature, 379, 304
- Srianand, R., & Kembhavi, A. 1997, ApJ, 478, 70
- Stocke, J.T., Morris, S.L., Gioia, I.M., Maccacaro, T., Schild, R., Wolter, A., Fleming, T.A., & Henry, J.P. 1991, ApJS, 76, 813

Table 1. Summary of the K -band Photometry of AX J131831+3341.

	K	$R - K$	$I - K$
	(mag)	(mag)	(mag)
Total	16.38	3.66	2.58
Nucleus	17.48	4.78	4.29
Total –Nucleus	16.87	3.32	2.17
Region A	18.56	3.34	2.54
Region B	18.43	3.71	2.49

Figure Captions

Fig. 1. K -band image of AX J131831+3341 with an effective exposure time of 1800 s (a). A model image (b) made by ellipse fitting and the residual image (c) are also shown. The field of view of the panels is $24'' \times 24''$. North is up and east is to the left. We show the surface brightness range from -3 times the standard deviation to $+9$ times the standard deviation as a gray scale with a linear scale. Regions A and B, where the magnitudes of the extended component were measured, are indicated with rectangles in panel a). The regions are the same as in Paper II.

Fig. 2. K -band profiles of AX J131831+3341 (thick solid line) in the southeastern (a) and northwestern (b) directions. The best-fit profiles are shown by the thick dashed lines. We plot 4 models in which the normalizations of the nuclear component and the extended component are changed independently with ± 0.2 mag with thin solid lines.

Fig. 3. $R-I$ and $I-K$ color-color diagram of the nuclear (filled square) and the extended (region A: filled triangle, region B: filled pentagon, total+nucleus: filled circle) components of AX J131831+3341. The open squares represents the colors of optically-selected QSOs at redshifts between 0.2 and 1.5 from Elvis et al. (1994). The pentagons show the colors of the power-law model with indices ($f_\nu = \nu^\alpha$) of -1.0 (top) and 0.0 (bottom). The dashed line indicates the expected color range for the $\alpha = -1$ power-law model with the absorption derived from X-ray spectrum ($A_V = 1 - 6$ mag). The absorption ($A_V > 3$ mag) estimated from the optical to X-ray flux ratio of the nuclear component only permits the thick region of the line. The tracks of the elliptical and disk models with ages of from 0.01 Gyr to 12 Gyr are indicated by the thick solid and dotted lines, respectively. The positions with the models at an age of 6 Gyr are marked with tick marks on each track. The arrow represents the effect of reddening with an A_V of 1 mag.

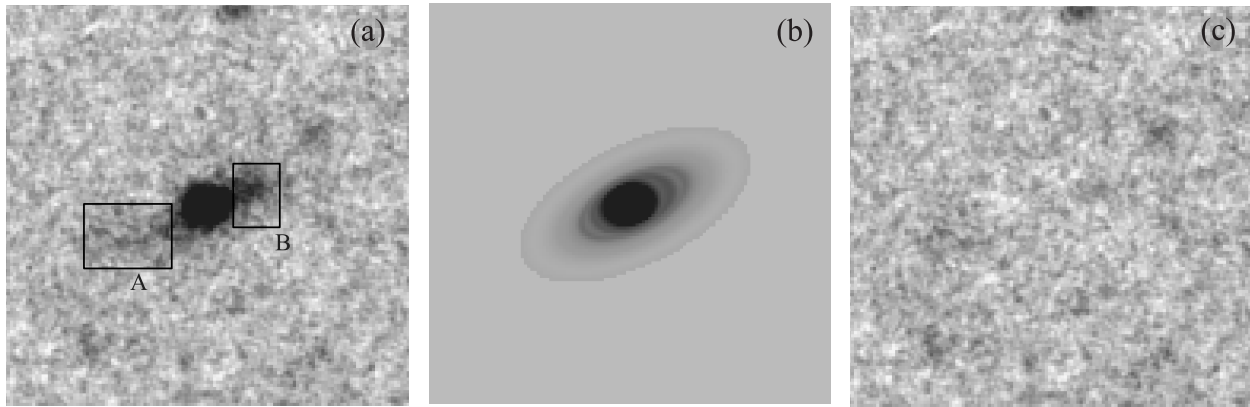


Fig. 1..

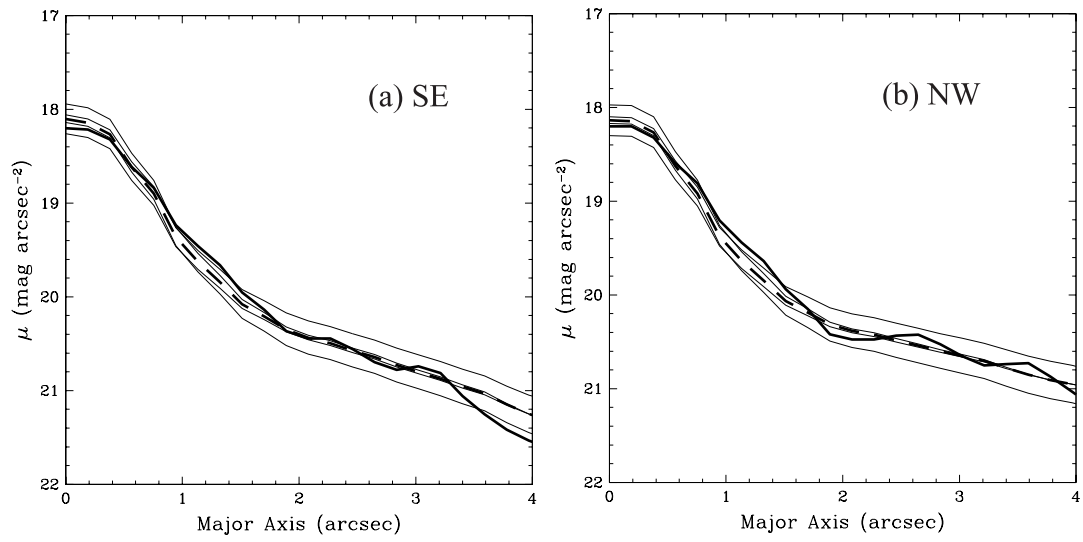


Fig. 2..

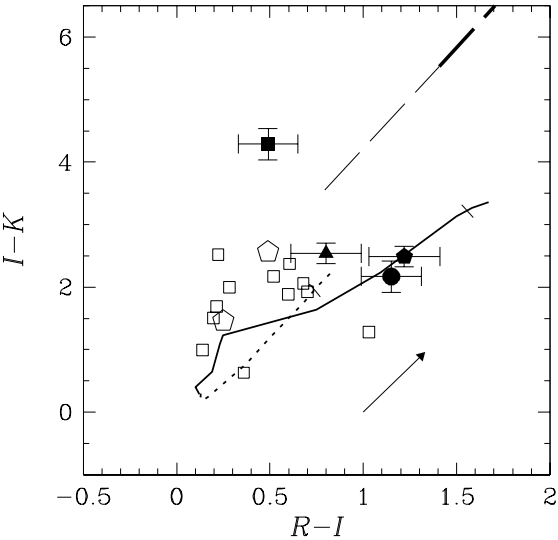


Fig. 3..